

INFORMATION TO USERS

This dissertation copy was prepared from a negative microfilm created and inspected by the school granting the degree. We are using this film without further inspection or change. If there are any questions about the content, please write directly to the school. The quality of this reproduction is heavily dependent upon the quality of the original material.

The following explanation of techniques is provided to help clarify notations which may appear on this reproduction.

1. Manuscripts may not always be complete. When it is not possible to obtain missing pages, a note appears to indicate this.
2. When copyrighted materials are removed from the manuscript, a note appears to indicate this.
3. Oversize materials (maps, drawings and charts are photographed by sectioning the original, beginning at the upper left hand corner and continuing from left to right in equal sections with small overlaps.

UMI[®]

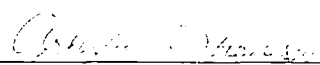
ProQuest Information and Learning
300 North Zeeb Road, Ann Arbor, MI 48106-1346 USA
800-521-0600

WETTING AND PENETRATION OF MULLITE
BY REACTIVE METALS

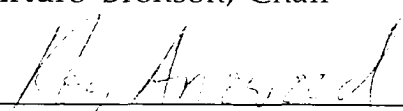
BRIAN PAUL HANSEN

Department of Metallurgical and Materials Engineering

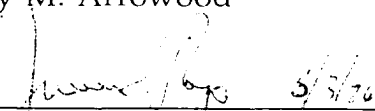
APPROVED:



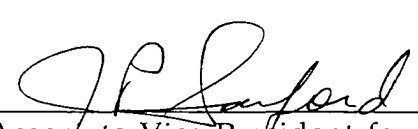
Arturo Bronson, Chair



Roy M. Arrowood



Javier Rojo



Associate Vice President for
Research and Graduate Studies

WETTING AND PENETRATION OF MULLITE
BY REACTIVE METALS

BY

BRIAN PAUL HANSEN, B.S.

THESIS

Presented to the Faculty of the Graduate School of
The University of Texas at El Paso
in Partial Fulfillment
of the Requirements
for the Degree of
MASTER OF SCIENCE

Department of Metallurgical and Materials Engineering
THE UNIVERSITY OF TEXAS AT EL PASO

July 1996

Acknowledgments

I would like to express my sincere appreciation to Dr. Arturo Bronson for his encouragement through out my college career and for the support through discussions and suggestion during this research. I also wish to thank Drs. Kevin Ewsuk and Ron Loehman at Sandia National Laboratories and Bill Fahrenholtz at the University of New Mexico for the opportunities and experience at Sandia National Laboratories and for support and encouragement through discussion and suggestion for this research. I want to also thank my fellow students and friends at UTEP and at Sandia during the summers, you know who you are, for making research fun and enjoyable. I especially wish to thank my parents for their support, encouragement and love. I finally wish to thank Sandia National Laboratories under contract DE-AC04-94AL85000 from the U.S. Department of Energy and the U.S. Department of Energy Office of Industrial Technology Advanced Materials Programs for the financial support for this research.

This thesis was submitted to the Graduate Committee on May 2, 1996.

Abstract

Interpenetrating phase $\text{Al}_2\text{O}_3/\text{Al}$ composites can form by reacting molten aluminum with mullite by the following reaction:



To characterize this reaction, wetting and penetration studies were conducted at 1100-1500°C in flowing deoxidized Ar. The contact angle of an Al sessile drop on dense and porous mullite was measured as a function of time at temperature. For the contact angles of Al on dense mullite at 1100 and 1200°C, the calculated liquid-solid surface tension (γ_{SL}) compare favorably with the reported γ_{SL} of Al on Al_2O_3 substrates.

The level of Al penetration and composite formation was measured on samples sectioned perpendicular to the reaction interface after cooling. Composite microstructures were characterized by using optical microscopy and an electron microprobe. Aluminum was found to wet dense mullite between temperatures of 1100 to 1500°C. Porous mullite, however, was only wetted by Al at temperatures above 1350°C. The penetration rate for Al into dense mullite preforms was 3 mm/hr with the penetration into porous mullite preforms being slightly higher at approximately 4 mm/hr.

The effect of alloying Al with Mg was evaluated by conducting comparable experiments with Al-Mg alloys 6061 and 5052 on both dense and porous mullite. It was found that the Al-Mg alloys slowed down the change in contact angles for both dense and porous mullite. The Al-Mg alloys showed a decrease in penetration into the mullite, both dense and porous, with increasing Mg content in the alloys. An additional phase, a

MgAl spinel (MgAl_2O_4), was identified by x-ray diffraction in composites formed from the Al 5052 alloy containing 2.5 wt% Mg.

The amounts of ceramic and metal phase in the composites can be controlled by processing temperature and preform porosity. The grain size of the composite phases increases with increasing processing temperature. Lower preform densities produce more metal phase in the composite.

PREVIEW

Table of Contents

Acknowledgments.....	iii
Abstract.....	iv
Table of Contents	vi
List of Tables.....	viii
List of Figures.....	ix
Chapters:	
1) Introduction.....	1
2) Literature Review.....	3
2.1) Background about CMC (ceramic matrix composites)	3
2.2) Wetting & Surface Energy	5
2.3) Phase Equilibria and Thermodynamics.....	8
3) Experimental Details.....	14
3.1) Materials.....	14
3.1.1) Mullite Powder	14
3.1.2) Reactive Metals.....	14
3.2) Ceramic Body Processing	15
3.3) Wetting and Penetration	16
3.3.1) Wetting Experiments.....	16
3.3.2) Penetration Experiments	19
3.4) Material Characterization.....	23
4) Results.....	25
4.1) Ceramic Bodies.....	25
4.2) Wetting and Penetration	25
4.2.1) Al Wetting	25
4.2.2) Alloy Wetting.....	27

4.2.3) Al Penetration.....	33
4.2.4) Alloy Penetration	33
4.2.5) Dipping	39
4.3) Characterization.....	42
5) Discussion	52
5.1) Thermodynamics of Al/mullite processing.....	52
5.1.1) Thermodynamics of Surfaces	52
5.1.2) Stability of Phases	55
5.2) Reactivity of Al/mullite processing.....	62
5.2.1) Proposed Mechanisms.....	62
5.2.2) Transport Phenomena	62
5.2.3) Processing Conditions	65
5.2.4) Wetting.....	66
5.2.5) Penetration.....	67
5.2.6) Penetration rate vs. $1/T$	68
5.3) Microstructure Characterization.....	69
6) Conclusions	76
References.....	78
Appendix	82
Curriculum Vitae	83

List of Tables

Table 3.1.1	Metal compositions (in weight percent) used for experiments.....	15
Table 3.3.1	Summary of wetting experiments conducted.	18
Table 3.3.2	Summary of penetration experiments conducted.....	23
Table 4.1.1	Densities of mullite preforms.....	25
Table 4.2.1	Penetration of Pure Al and Al 5052 into dense mullite at 1200°C, and porous mullite at 1400°C after 1 hour reaction.....	42
Table 5.1.1	The calculated liquid/solid surface tensions (γ_{SL}) for Al on Al ₂ O ₃ from Young's equation.....	54

List of Figures

Figure 2.1	Wetting of a solid by a liquid.....	7
Figure 2.2	Non-wetting of a solid by a liquid.....	7
Figure 2.3	Al ₂ O ₃ -SiO ₂ phase diagram showing mullite composition at 72 wt% alumina.....	10
Figure 2.4	Al-Si phase diagram.....	11
Figure 2.5	Al-Mg phase diagram.....	12
Figure 2.6	Mg-Si phase diagram showing the Mg ₂ Si intermetallic	13
Figure 3.1.	Schematic of high temperature wetting furnace	17
Figure 3.2.	Cross-section showing the measurement for maximum penetration depth (d) in a wetting experiment sample.....	20
Figure 3.3	Apparatus for dipping experiments.....	21
Figure 3.4.	Cross-section showing the measurement for maximum penetration depth (d) in a dipping experiment sample	22
Figure 4.1	Time dependent contact angles of pure Al on dense mullite (>80% theoretical density) at 1200 and 1500°C	26
Figure 4.2	Cross-section of pure Al reacted with dense mullite for one hour a.) at 1200°C and b.) at 1500°C	28
Figure 4.3	Time dependent contact angles of pure Al on porous mullite (<65% theoretical density) at 1200, 1300, 1400, and 1500°C	29
Figure 4.4	Cross-section of pure Al reacted with porous mullite for one hour a.) at 1200°C and b.) at 1500°C	30
Figure 4.5	Time dependent contact angles measured for Al alloys on 99% dense mullite at 1100°C.....	31

Figure 4.6.	Cross-sections of metals, a.) pure Al, b.) 6061, and c.) 5052 reacted with 99% dense mullite for 1 hour at 1100°C showing the hemispherical sessile drop of metal on top and the hemispherical composite reaction area within the original, rectangular mullite substrate	32
Figure 4.7	Time dependent contact angles of Al alloys on porous mullite (60% dense) at 1400°C.....	34
Figure 4.8	Cross-sections of metals, a.) pure Al, b.) 6061, and c.) 5052 reacted with porous mullite (60% dense) for 1 hour at 1400°C	35
Figure 4.9	Effect of temperature on the penetration depth of Al into 84 and 99% dense mullite after reacting for one hour	36
Figure 4.10	Effect of temperature on the penetration depth of Al into porous mullite (54, 55, 56, and 60% dense) after reacting for one hour	37
Figure 4.11	Penetration depth of Al alloys into 99% dense mullite after reacting at 1100°C for one hour	38
Figure 4.12	Penetration depth of Al alloys into porous mullite (60% dense) after reacting at 1400°C for one hour	40
Figure 4.13	Penetration depth for porous mullite (60% dense) dipped into pure Al at 1500°C as a function of time	41
Figure 4.14	XRD spectra for pure Al reacted with 99% dense mullite showing Al ₂ O ₃ (AO), Al (A), and Si (S)	43
Figure 4.15	XRD spectra for Pure Al reacted with porous mullite (60% dense) showing Al ₂ O ₃ (AO), Al (A), and Si (S) phases	44
Figure 4.16	XRD spectra for Al alloys reacted with porous mullite (60% dense) showing Al ₂ O ₃ (AO), Al (A), and Si (S). The Al 5052 also shows a MgAl ₂ O ₄ (MA) spinel phase.....	45
Figure 4.17	Microstructure of composite formed by reacting pure Al with 99% dense mullite at 1200°C. The dark areas are the Al ₂ O ₃ and the light areas are the Al	47

Figure 4.18	Microstructure of composite formed by reacting pure Al with 99% dense mullite at 1500°C. The dark areas are the Al_2O_3 and the light areas are the Al	48
Figure 4.19	Microstructure of composite formed by reacting pure Al with porous mullite (60% dense) at 1500°C. The dark areas are the Al_2O_3 , dark gray areas are the Si and the light gray areas the Al	49
Figure 4.20	a.) SEM image of a composite formed by reacting pure Al with porous mullite (60% dense) at 1500°C showing the Al_2O_3 phase (raised) and the metal phases (Al and Si). b.) Si map of the same area in a).....	50
Figure 5.1	Activity of dissolved oxygen (Q) in Al at the Al/ Al_2O_3 /Si equilibrium and at the Ti/TiO equilibrium (oxygen activity was calculated by using Chang's data [29]).....	56
Figure 5.2	Free energy diagram for mullite showing alumina is more stable than mullite (calculated from thermodynamic data in Turkdogan [30]).....	57
Figure 5.3	For a temperature of 1400 K, Al-Si-O ternary phase diagram showing the invariant region for the reaction products (constructed from Massalski's binary diagrams [25])	59
Figure 5.4	Log $p\text{O}_2$ increases with increasing temperature in the Al_2O_3 /Al/Si system (oxygen potential was calculated by using Turkdogan's data [30]).....	60
Figure 5.5	Al-Si-O ternary phase diagram showing the equal shaded areas for the mass balance (constructed from Massalski's binary diagrams [25]).....	61
Figure 5.6	Illustration for Darcy's Law in the dipping experiments, P_o = atm pressure, P the pressure in the melt and h the height.....	64
Figure 5.7	Penetration depth as a function of $1/T$ for porous mullite for a reaction time of 1 hour.....	70

Figure 5.8	Comparison between a.) SE and b.) BSE images of a composite formed by reacting pure Al with porous mullite (60% dense) at 1500°C showing the Al_2O_3 phase (raised) and the metal phases (Al and Si)	72
Figure 5.9	Free energy diagram with MgAl spinel and MgO (calculated from thermodynamic data in Turkdogan [30])	74
Figure 5.10	Al_2O_3 -MgO-SiO ₂ ternary phase diagram	75

PREVIEW

Chapter 1

Introduction

Composites are materials made up of two or more phases which together improve the combination of physical properties of the original parent materials. [1-2] The reinforcement phase consisting of particles, fibers or different phases is stronger or tougher than the matrix material which yields to the improved properties. Strength, fracture toughness and density are just some of the improved properties that make composites attractive in many applications. Composite materials have been grouped into categories based on their matrix material consisting of polymer matrix composites (PMC), metal matrix composites (MMC) and ceramic matrix composites (CMC), which have existed for some time, but just recently have come into the spot light. For example, in MMC's, ceramic fibers are added to the metal matrix to strengthen and increase toughness. Similarly with ceramics, depending on the desired properties, ceramic fibers are added to a ceramic matrix to increase strength, or a metal phase is added to the ceramic matrix to improve the ductility and fracture toughness of the ceramic. The deficiencies of composites are in their fabrication. Many composites are expensive and difficult to product. But with the increased use of these composites in the aircraft, automobile, and leisure industries, just to name a few, the field of composite fabrication has grown to help solve the deficiencies of composite processing.

This thesis investigates the process for fabricating one of these ceramic matrix composites -- alumina/aluminum composites. The

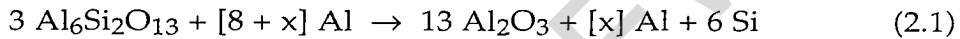
objective of this research was to determine the controlling factors in the formation of alumina/aluminum composites by the reactive metal penetration (RMP) method. In reactive metal penetration, a ceramic preform (i.e. mullite) reacts with liquid metal (i.e. aluminum) to form a ceramic matrix composite. Because liquid metal must penetrate along the pores and/or grain boundaries as well as the ceramic grains, the investigation developed into studying the contact angle, reaction front and microstructure. The contact angle between the ceramic and the liquid metal depends on the surface tension. However, the contact angle measurements are complicated because interfacial reactions are also involved between the mullite and liquid metal. The reaction front or the penetration of the liquid into the mullite depends on the reactivity of the mullite with the liquid aluminum. The microstructure of the alumina/aluminum provides a clue for evaluating the extent of the reactions. The diffusion of the reacting species is complicated by the interfaces and pores through which Si and O must transfer. In the present study, mass transfer was considered secondary compared to the effects of the surface tension and reactivity along the metal/mullite interface. Hence, the focus of the research in this thesis is the surface reactivity and the microstructural features of the liquid metal penetrating the ceramic preform.

Chapter 2

Literature Review

2.1) Background about CMC (ceramic matrix composites)

Loehman et al. [3] reported on reactive metal penetration (RMP) for processing ceramic-metal composites which are near net-shape. The process consists of a liquid metal (e.g, aluminum) reacting with a ceramic (e.g, aluminosilicate) to form an alumina/aluminum composite according to Reaction 2.1.



They investigated the processing of composites formed from wetting studies, similar to those which will be discussed in this thesis, and by immersing a ceramic preform into molten aluminum. Composites were also formed by hot pressing mullite and aluminum powders. Dense mullite preforms were first used to form the composites [3-5] and then later porous preforms were also used in forming the $\text{Al}_2\text{O}_3/\text{Al}$ composites [6]. The composites that were formed from either preform density produced dense composites of a 3-D network of interconnected ceramic and metal phases. The dense mullite reacted with Al developed approximately 15% metal phase and 85% ceramic phase in the composites upon completion of the reaction. [3-5] Similarly after the reaction with the porous mullite, the composites showed 49 to 50% metal phase in the composites. [6] The bend strength of the composites was approximately

250 MPa. The additions of the metal phase to the ceramic improve the fracture toughness to $\geq 6 \text{ MPa}\cdot\sqrt{\text{m}}$ compared to $2 \text{ MPa}\cdot\sqrt{\text{m}}$ for dense mullite without a decrease in strength.

Ceramic-metal composites can also be made by pressure infiltration in which liquid metal is pressurized into the ceramic preform. [7] The ceramic reinforcement is the most difficult part of the process because the spaces between the reinforcement (e.g, fibers and particles) and the metal change with application of the infiltration pressure. In addition, the reinforcement preforms must be evacuated before the metal can be pushed into the preform so gas pockets do not form in the composite, which would affect the properties.

Lanxide has patented a liquid-gas reaction process to produce ceramic-metal composites called the DIMOX™ or direct metal oxidation process. [8] In this process, molten metal is oxidized to form the composite. A preform is placed on top of a metal pool, and metal is drawn up into the preform where it oxidizes as it grows through the preform. Lanxide has used the process to form alumina/aluminum composites from aluminum and Al alloys as well as other ceramic-metal composites such as Zr reacting with boron carbide (BC) to form ZrB_2 & ZrC . [9-11]

Matsuo and Inaba [12] and Breslin, et al. [13-14] have produced composites by reacting amorphous silica and molten aluminum. Matsuo and Inaba [12] composites are made of a mutually interpenetrating structure of about 70 wt% alumina and about 30 wt% metal phase consisting of Al and Si. Their $\text{Al}_2\text{O}_3/\text{Al}/\text{Si}$ composites were formed at temperatures between 900 and 1000°C. Breslin et al. [13-14] also reacted Al

with amorphous silica to form $\text{Al}_2\text{O}_3/\text{Al-Si}$ composites. Both research groups reported improvements in bend strength and other physical properties for the $\text{Al}_2\text{O}_3/\text{Al/Si}$ composites.

2.2) Wetting & Surface Energy

To form ceramic-metal composites, wetting of the metal on the ceramic preforms is desired. A method to study wetting involves a liquid bead on the solid substrate to form a sessile drop whose equilibrium shape is determined by a balance of surface energies. The contact angle (θ) is the angle formed between the solid/liquid interface and the tangent of the liquid/vapor interface that emanates from the triple point, as shown in Figure 2.1. For wetting, the energies must favor replacing liquid/vapor interfacial area with lower solid/liquid interfacial areas. If the contact angle is less than 90° , the liquid is in a state of partial wetting or the onset of wetting the surface. Complete wetting is when the contact angle is or approaches zero (0°). At this point the liquid spreads across the surface of the solid by spreading across the substrate. Similarly if the thermodynamics of the system favor creating solid/vapor interfacial area at the expense of the solid/liquid interfacial area the liquid is non-wetting (Figure 2.2). In the non-wetting case, the contact angle is greater than 90° and the liquid moves towards the equilibrium shape of a sphere. Pask and Tomisa [15] describe wetting as when the solid interfacial energy is lowered when in contact with a liquid and the surface will tend to be covered by the liquid. If the opposite case happens, when the solid interfacial energy is increased when in contact with the liquid, the solid/liquid area is

minimized and the solid is not wetted. When the liquid and solid are in equilibrium or a steady-state condition, Young's equation (Equation 2.2) can be used to express the effect of the interfacial energies on the contact angle.

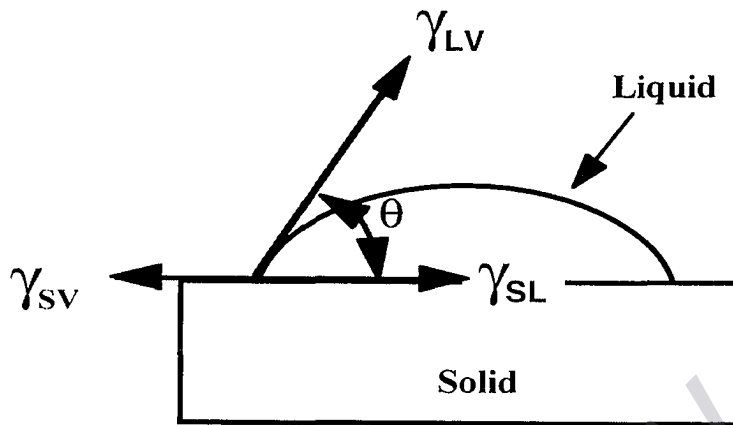
$$\gamma_{SV} - \gamma_{SL} = \gamma_{LV} \cos \theta \quad (2.2)$$

The liquid surface tension (γ_{LV}) is controlled by the driving force for wetting ($\gamma_{SV} - \gamma_{SL}$). To lower the contact angle (θ) the interfacial energies in Young's equation can be manipulated. The lowering of γ_{LV} causes $(\gamma_{SV} - \gamma_{SL})/\gamma_{LV}$ to increase, and thus a lower contact angle (θ). For the condition of $\theta < 90^\circ$, or wetting, then γ_{SV} is greater than γ_{SL} . In a non-wetting condition for $\theta > 90^\circ$, γ_{SV} is less than γ_{SL} . Therefore to lower the contact angle (θ) a high γ_{SV} and a low γ_{LV} are desired.

In the presence of a reaction between the liquid drop and substrate, Young's equation is modified to include the contribution of the free energy of reaction, which contributes to the driving force for wetting;

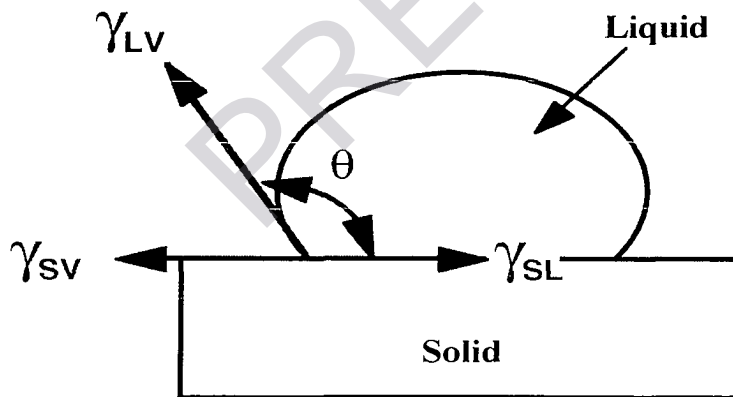
$$\gamma_{SV} - \left(\gamma_{SL} + \frac{\Delta G_R}{dA_s} \right) \geq \gamma_{LV} \cos \theta \quad (2.3)$$

where A_s is the surface area of the drop and ΔG_R represents the Gibbs free energy of the reaction [15]. In the presence of a reaction the expansion of the liquid drop on the solid is defined as spreading. This spreading is related to the dynamic decrease in the contact angle. A reaction between the liquid and the solid can be enhanced by an increase in temperature.



$$\gamma_{SV} > \gamma_{SL} + \gamma_{LV}$$

Figure 2.1 Wetting of a solid by a liquid. [15]



$$\gamma_{SV} < \gamma_{SL} + \gamma_{LV}$$

Figure 2.2 Non-wetting of a solid by a liquid. [15]